

Interacting model of new agegraphic dark energy: Cosmological evolution and statefinder diagnostic

Li Zhang, Jinglei Cui, Jingfei Zhang, and Xin Zhang

Department of Physics, College of Sciences, Northeastern University, Shenyang 110004, China

The statefinder diagnostic is a useful method for distinguishing different dark energy models. In this paper, we investigate the new agegraphic dark energy model with interaction between dark energy and matter component by using statefinder parameter pair $\{r, s\}$ and study its cosmological evolution. We plot the trajectories of the new agegraphic dark energy model for different interaction cases in the statefinder plane. As a result, the influence of the interaction on the evolution of the universe is shown in the statefinder diagrams.

I. INTRODUCTION

Recent astronomical observations of type Ia supernovae (SNIa) indicate that the universe is undergoing an accelerating expansion [1, 2]. This cosmic acceleration has also been confirmed by other observations, such as observations of large scale structure (LSS) [3, 4] and measurements of the cosmic microwave background (CMB) anisotropy [5, 6]. Nowadays the most well-accepted idea is that a mysterious dominant component — dark energy — with large enough negative pressure is responsible for this the cosmic acceleration. Despite the fact that the cosmological origin of dark energy remains enigmatic at present, physicists have to face the intriguing physical problem and try to understand the ultimate nature of dark energy. Among all theoretical models, the preferred candidate of dark energy is the Einstein’s cosmological constant Λ . The simplest cosmological model is the so-called Λ CDM (or LCDM) model, which consists of a mixture of the cosmological constant Λ and the cold dark matter (CDM). The LCDM model provides an excellent explanation for the acceleration of the universe and the existing observational data. However, the cosmological constant faces two difficulties, namely, the “fine-tuning” problem and the “cosmic coincidence” problem. The former asks why the cosmological constant observed today is so much smaller than the Planck scale, while the latter asks why the energy densities of dark energy and matter are on the same order today. Theorists have made lots of efforts to try to resolve the cosmological constant problem but all these efforts have turned out to be unsuccessful.

In order to alleviate or even solve these two problems, many dynamical dark energy models have been proposed, whose equation of state is no longer a constant but slightly evolves with time. The dynamical dark energy scenario is often realized by some scalar-field mechanism which suggests that the energy with negative pressure is provided by a scalar field evolving down a proper potential. A lot of scalar field dark

energy models have been studied, such as quintessence, K -essence, tachyon, phantom and quintom etc.. Besides, some interacting models have been discussed in many works to help understand or alleviate the coincidence problem by considering the possible interaction between dark energy and dark matter owing to their unknown nature. For reviews of dark energy, see, e.g., Ref. [7].

On the other hand, in various dark energy models, the property of dark energy is strongly model-dependent. In order to be capable of differentiating those competing cosmological dark energy scenarios, a sensitive diagnostic for the many dark energy models is a must. For characterizing the expansion history of the universe, one defines the geometric parameters $H = \dot{a}/a$ and $q = -\ddot{a}/aH^2$, namely, the Hubble parameter and the deceleration parameter; here $a(t)$ is the scale factor of the Friedmann-Robertson-Walker (FRW) universe. It is clear that $\dot{a} > 0$ means that the universe is undergoing an expansion and $\ddot{a} > 0$ means the universe is experiencing an accelerated expansion. The cosmic acceleration indicates that q should be less than zero. However the deceleration parameter on its own does not characterize the current acceleration phase uniquely. The presence of a fairly large degeneracy in q is reflected in the fact that rival dark energy models can give rise to the same value of q_0 at the present time. Under such circumstances, a robust diagnostic of dark energy, statefinder parameter pair $\{r(z), s(z)\}$, was introduced by Sahni et al. [8] and Alam et al. [9]. In addition, more recently, two new diagnostics of dark energy, Om and acceleration probe \bar{q} , were introduced by Sahni, Shafieloo and Starobinsky [10].

The statefinder probes the expansion dynamics of the universe through high derivatives of the scale factor \ddot{a} and $\ddot{\ddot{a}}$ and is a natural next step beyond the Hubble parameter H depending on \dot{a} and the deceleration parameter q depending on \ddot{a} . The statefinder pair $\{r, s\}$ is defined as

$$r \equiv \frac{\ddot{\ddot{a}}}{aH^3}, \quad (1)$$

$$s \equiv \frac{r - 1}{3(q - \frac{1}{2})}. \quad (2)$$

It is a ‘‘geometrical’’ diagnostic, in the sense that it is constructed from a space-time metric directly, and it is more universal than ‘‘physical’’ variables, which depend upon properties of physical fields describing dark energy. So, in order to see the qualitatively different cosmological evolution behaviors of dark energy models in degeneracy of H_0 and q_0 , we can plot statefinder parameter diagrams corresponding to these dark energy models by theoretical calculation. As a reference the spatially flat Λ CDM scenario corresponds to a fixed point $\{r, s\} = \{1, 0\}$ in this diagram. Departure of a given dark energy model from this fixed point provides a good way of establishing the ‘‘distance’’ of this model from the Λ CDM [9]. On the other hand, the statefinder can also be extracted from data coming from SuperNova Acceleration Probe (SNAP) type experiments [8, 9]. Therefore, the statefinder diagnostic combined with future SNAP observations may

possibly be used to discriminate between different dark energy models. In this paper, we just apply the statefinder diagnostic to the new agegraphic dark energy (NADE) model.

We will investigate the features of the NADE model with interaction with matter component from the statefinder view point. In Sec. II, we will briefly review the NADE model and introduce an interacting model of NADE. In Sec. III, we will study the cosmological evolution of the interacting NADE model. In Sec. IV, we will apply the statefinder diagnostic to the interacting NADE model. In the last section we will give conclusions.

II. AN INTERACTING MODEL OF NEW AGEGRAPHIC DARK ENERGY

First, let us review the NADE model. So far, we cannot confirm if dark energy imitates as a cosmological constant or a dynamical field. Generally, theorists believe that we cannot entirely understand the nature of dark energy before a complete theory of quantum gravity is established [11]. However, we still can make some efforts to probe the properties of dark energy according to some principle of quantum gravity. The holographic dark energy model [12] and the agegraphic dark energy model [13] are examples, possessing some significant features of quantum gravity. The former stems from the holographic principle and the latter is constructed in light of the Károlyházy relation [14] and corresponding energy fluctuations of space-time. In this paper, we just focus on the agegraphic dark energy model.

In general relativity, one can measure the space-time without any limit to accuracy. However, in the quantum mechanics, the well-known Heisenberg uncertainty relation puts a limit of accuracy in these measurements. Following the line of quantum fluctuations of spacetime, Károlyházy and collaborators [14] made an interesting observation concerning the distance measurement for Minkowski spacetime through a light-clock Gedanken experiment; namely, the distance t in Minkowski space-time cannot be known to a better accuracy than

$$\delta t = \lambda t_p^{2/3} t^{1/3}, \quad (3)$$

where λ is a dimensionless constant of order unity. We use the units $\hbar = c = k_B = 1$ throughout this paper. Thus, one can use the terms like length and time interchangeably, whereas $l_p = t_p = 1/m_p$ with l_p , t_p and m_p being the reduced Planck length, time and mass, respectively.

The Károlyházy relation (3) together with the time-energy uncertainty relation enables one to estimate a quantum energy density of the metric fluctuations of Minkowski space-time. Following Refs. [15, 16], with respect to Eq. (3) a length scale t can be known with a maximum precision δt , determining thereby a minimal detectable cell $\delta t^3 \sim t_p^2 t$ over a spatial region t^3 . Such a cell represents a minimal detectable unit of

space-time over a given length scale t . If the age of the Minkowski space-time is t , then over a spatial region with linear size t (determining the maximal observable patch) there exists a minimal cell δt^3 , the energy of which due to the fact that the time-energy uncertainty relation cannot be smaller than

$$E_{\delta t^3} \sim t^{-1}. \quad (4)$$

Therefore, the energy density of metric fluctuations of Minkowski space-time is given by

$$\rho_q \sim \frac{E_{\delta t^3}}{\delta t^3} \sim \frac{1}{t_p^2 t^2} \sim \frac{m_p^2}{t^2}. \quad (5)$$

Based on the energy density (5), the so-called agegraphic dark energy model was proposed in Ref. [13]. In this model, as the most natural choice, the time scale t in Eq. (5) is chosen to be the age of the universe

$$T = \int_0^a \frac{da}{Ha}, \quad (6)$$

where a is the scale factor of our universe, and H is the Hubble parameter. Thus, the energy density of the agegraphic dark energy is given by [13]

$$\rho_q = \frac{3n^2 m_p^2}{T^2}, \quad (7)$$

where the numerical factor $3n^2$ has been introduced to parameterize some uncertainties, such as the species of quantum fields in the universe, or the effect of curved space-time (since the energy density is derived for Minkowski space-time). Obviously, since the present age of the universe $T_0 \sim H_0^{-1}$ (the subscript 0 indicates the present value of the corresponding quantity), the present energy density of the agegraphic dark energy explicitly meets the observed value naturally, provided that the numerical factor n is of order unity. In addition, by choosing the age of the universe rather than the future event horizon as the length measure, the drawback concerning causality in the holographic dark energy model does not exist in the agegraphic dark energy model [13].

If we consider a spatially flat FRW universe containing agegraphic dark energy and pressureless matter, the corresponding Friedmann equation reads

$$H^2 = \frac{1}{3m_p^2} (\rho_m + \rho_q). \quad (8)$$

It is convenient to introduce the fractional energy densities $\Omega_i \equiv \rho_i/3m_p^2 H^2$ for $i = m$ and q . From Eq. (7), it is easy to find

$$\Omega_q = \frac{n^2}{H^2 T^2}. \quad (9)$$

Obviously, $\Omega_m = 1 - \Omega_q$ from Eq. (8). By using Eqs. (6)–(9) and the energy conservation equation $\dot{\rho}_m + 3H\rho_m = 0$, we obtain the equation of motion for Ω_q ,

$$\Omega'_q = \Omega_q \left(1 - \Omega_q\right) \left(3 - \frac{2}{n} \sqrt{\Omega_q}\right), \quad (10)$$

where the prime denotes the derivative with respect to $N \equiv \ln a$. Evidently, from the energy conservation equation $\dot{\rho}_q + 3H(\rho_q + p_q) = 0$, as well as Eqs. (7) and (9), it is easy to find that the equation of state (EoS) of the agegraphic dark energy $w_q \equiv p_q/\rho_q$ is given by [13]

$$w_q = -1 + \frac{2}{3n} \sqrt{\Omega_q}. \quad (11)$$

However, there are some inner inconsistencies in this model; for details see Ref. [17]. Therefore a new version of the agegraphic dark energy model was proposed to resolve the difficulties by replacing the timescale T in Eq. (6) with the conformal time η [18, 19]. This new version is often called the “new agegraphic dark energy” model. In this new version, the energy density of the agegraphic dark energy reads

$$\rho_q = \frac{3n^2 m_p^2}{\eta^2}, \quad (12)$$

where

$$\eta \equiv \int_0^t \frac{dt}{a} = \int_0^a \frac{da}{a^2 H} \quad (13)$$

is the conformal age of the universe. The corresponding fractional energy density reads

$$\Omega_q = \frac{n^2}{H^2 \eta^2}. \quad (14)$$

Again we consider a flat FRW universe containing the new agegraphic dark energy and matter. By using Eqs. (8), (12)–(14) and the energy conservation equation $\dot{\rho}_m + 3H\rho_m = 0$, we find that the equation of motion for Ω_q is

$$\Omega'_q = \Omega_q \left(1 - \Omega_q\right) \left(3 - \frac{2}{n} \frac{\sqrt{\Omega_q}}{a}\right). \quad (15)$$

From the energy conservation equation $\dot{\rho}_q + 3H(\rho_q + p_q) = 0$, as well as Eqs. (12) and (14), it is easy to find that the EoS of the new agegraphic dark energy is given by

$$w_q = -1 + \frac{2}{3n} \frac{\sqrt{\Omega_q}}{a}. \quad (16)$$

The NADE model has been studied extensively; see, e.g., Refs. [18–20]. In this paper, furthermore, we shall extend the NADE model by including the interaction between the agegraphic dark energy and matter. We will see that the interaction can significantly change the cosmological evolution. Assuming that the

agegraphic dark energy and matter exchange energy through interaction term Q , the continuity equations become

$$\dot{\rho}_q + 3H(\rho_q + p_q) = -Q, \quad (17)$$

$$\dot{\rho}_m + 3H\rho_m = Q, \quad (18)$$

where Q can be assumed as some special forms. For convenience, here we consider only the following particular interaction forms:

$$Q = \begin{cases} 3\alpha_1 H \rho_q \\ 3\alpha_2 H \rho_m \\ 3\alpha_3 H (\rho_q + \rho_m) \end{cases}. \quad (19)$$

Differentiating Eq. (14) with respect to $\ln a$ and using Eq. (13), we get

$$\Omega'_q = \Omega_q \left(-2 \frac{\dot{H}}{H^2} - \frac{2}{na} \sqrt{\Omega_q} \right). \quad (20)$$

Differentiating Eq. (8) with respect to time t and combining Eqs. (12)–(14), (17) and (18), one can easily find

$$- \frac{\dot{H}}{H^2} = \frac{3}{2} (1 - \Omega_q) + \frac{\Omega_q^{3/2}}{na} - \frac{Q}{6m_p^2 H^3}. \quad (21)$$

Therefore, we obtain the equation of motion for Ω_q ,

$$\Omega'_q = \Omega_q \left[(1 - \Omega_q) \left(3 - \frac{2}{na} \sqrt{\Omega_q} \right) - Q_1 \right], \quad (22)$$

where

$$Q_1 \equiv \frac{Q}{3m_p^2 H^3}. \quad (23)$$

From Eqs. (12), (14) and (17), we get the EoS of the interacting NADE as

$$w_q = -1 + \frac{2}{3na} \sqrt{\Omega_q} - Q_2, \quad (24)$$

where

$$Q_2 \equiv \frac{Q}{3H\rho_q}. \quad (25)$$

It is easy to see that Eqs. (22) and (24) reduce to Eqs. (15) and (16) in the case of $Q = 0$ (i.e. without interaction). Therefore, we get Ω'_q and EoS of the NADE model for the cases with and without interaction. Next, let us look into some properties of this model.

Consider first the properties of the new agegraphic dark energy without interaction. In the radiation-dominated epoch, $w_q = -1/3$ whereas $\Omega_q = n^2 a^2$; in the matter-dominated epoch, $w_q = -2/3$ whereas $\Omega_q = n^2 a^2/4$; eventually, the new agegraphic dark energy dominates; in the late time $w_q \rightarrow -1$ when $a \rightarrow \infty$, the new agegraphic dark energy mimics a cosmological constant. (See Ref. [18] for more details.) It is worth noting that this NADE model without interaction is a single-parameter model because of its special analytic features in the radiation-dominated and matter-dominated epochs. Concretely, in the matter-dominated epoch, $\Omega_q = n^2 a^2/4 = n^2(1+z)^{-2}/4$, where $z = a^{-1} - 1$ is the redshift. Therefore, $\Omega_q(z_{ini}) = n^2(1+z_{ini})^{-2}/4$ can be used as the initial condition to solve the differential equation of Ω_q at any z_{ini} provided that it is sufficiently deep into the matter-dominated epoch. We choose here $z_{ini} = 2000$ in the initial condition, just as in Ref. [19]. If n is given, we can obtain Ω_q from Eq. (22) by using the initial condition. Then, all other physical quantities, such as $\Omega_m(z) = 1 - \Omega_q(z)$ and $w(z)$, can be obtained correspondingly.

When interaction Q is included, the situation is changed. For NADE model without interaction ($Q = 0$), the EoS w_q is always larger than -1 and cannot cross the phantom divide $w = -1$, see Eq. (16). However, if the interaction $Q \neq 0$ and $Q > 0$, one can see that w_q can be smaller than -1 or larger than -1 from Eq. (24). This means that the EoS w_q can possibly cross the phantom divide in the interacting NADE model. In this case, it should be pointed out that the initial condition $\Omega_q(z_{ini}) = n^2(1+z_{ini})^{-2}/4$ with $z_{ini} = 2000$ can also be used. In matter-dominated epoch, the contribution of dark energy to the cosmological evolution is negligible so that the impact of dark energy on matter can be ignored. That is to say, dark energy cannot affect the evolution behavior of matter at early times in spite of the existence of the interaction. So, the mentioned initial condition $\Omega_q(z_{ini}) = n^2(1+z_{ini})^{-2}/4$ with $z_{ini} = 2000$, is still proper in solving the differential equation of Ω_q in the case of $Q \neq 0$. In the next section, we will discuss the cosmological evolution of the interacting NADE model.

III. COSMOLOGICAL EVOLUTION OF THE INTERACTING NADE MODEL

For the interacting NADE model, the continuity equations for dark energy and matter can be written as Eqs. (17) and (18), where the interaction between dark energy and matter component is characterized by Q . It is convenient to define the effective EoSs for dark energy and matter as

$$w_q^{(e)} = w_q + \frac{Q}{3H\rho_q}, \quad (26)$$

$$w_m^{(e)} = -\frac{Q}{3H\rho_m}. \quad (27)$$

According to the definition of the effective EoSs, the continuity equations for dark energy and matter can be re-expressed in forms of energy conservation,

$$\dot{\rho}_q + 3H(1 + w_q^{(e)})\rho_q = 0, \quad (28)$$

$$\dot{\rho}_m + 3H(1 + w_m^{(e)})\rho_m = 0. \quad (29)$$

Taking aforementioned three cases of interaction, one can obtain

$$w_m^{(e)} = \begin{cases} \frac{-\alpha_1 \Omega_q}{(1 - \Omega_q)} & \text{for } Q = 3\alpha_1 H \rho_q \\ -\alpha_2 & \text{for } Q = 3\alpha_2 H \rho_m \\ -\alpha_3 \left[1 + \frac{\Omega_q}{(1 - \Omega_q)} \right] & \text{for } Q = 3\alpha_3 H (\rho_q + \rho_m) \end{cases}. \quad (30)$$

Considering a spatially flat FRW universe with dark energy ρ_q and matter ρ_m , the Friedmann equation can be expressed as

$$H(a) = H_0 E(a), \quad (31)$$

where

$$E(a) = \left[\frac{(1 - \Omega_{q0}) e^{-3 \int_1^a (1 + w_m^{(e)}) d \ln a}}{1 - \Omega_q} \right]^{1/2}. \quad (32)$$

We plot the cosmological evolution of $E(z)$ in Figs. 1 and 2. First, we fix the interaction parameter α_i ($i = 1, 2, 3$, respectively) and vary the model parameter n . In Fig. 1, we show four cases, namely, the case without interaction ($\alpha = 0$), the case of $Q = 3\alpha_1 H \rho_q$ with $\alpha_1 = 0.1$, the case of $Q = 3\alpha_2 H \rho_m$ with $\alpha_2 = 0.08$, and the case of $Q = 3\alpha_3 H (\rho_q + \rho_m)$ with $\alpha_3 = 0.06$. For each case, we vary the parameter n and take $n = 2, 3, 4$, and 5 , respectively. From this figure, we see that for different interaction cases the cosmic evolution trends seem quite similar, i.e., the smaller value the parameter n is taken, the bigger value the Hubble expansion rate $E(z)$ gets. Next, we fix the model parameter n (we take the case of $n = 3$) and vary the interaction parameter α_i . In Fig. 2, we show the three interaction cases. Also, we see from this figure that the cosmic evolution trends are quite similar for these three interaction cases. The smaller the interaction parameter α_i is taken, the bigger the Hubble expansion rate $E(z)$ can reach. Therefore, from the above analysis, we find that both the parameters, n and α_i , can impact the cosmic expansion history in the interacting NADE model.

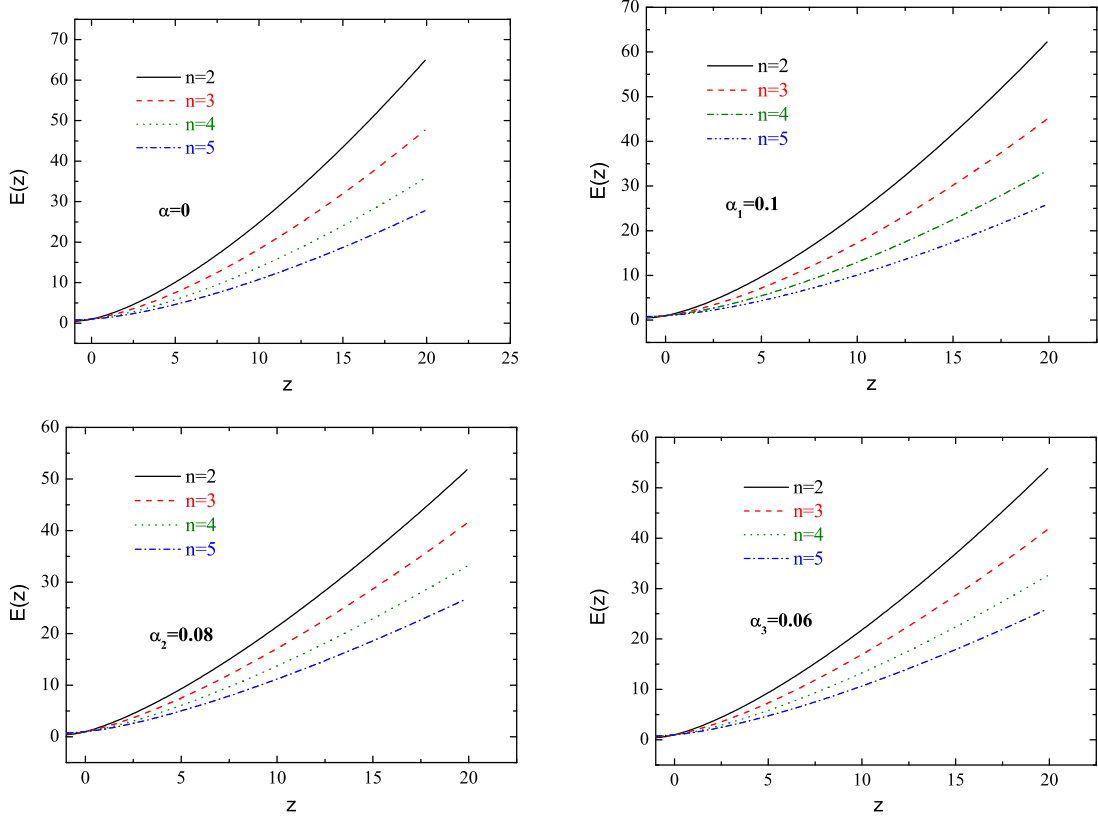


FIG. 1: The evolution of $E(z)$ for the interacting NADE model with the parameter $n = 2, 3, 4$ and 5 , respectively.

IV. STATEFINDER DIAGNOSTIC FOR THE INTERACTING NADE MODEL

Now, let us switch to the statefinder diagnostic. In this section, we will apply it to the interacting NADE model introduced in the previous section. For other works on the statefinder diagnostic to dark-energy models, see, e.g., Refs. [8, 9, 21].

First, we will derive the general form of the statefinder parameters for interacting dark energy models. The total EoS is defined as $w_{tot} \equiv p_{tot}/\rho_{tot} = -1 - \frac{2}{3}\frac{\dot{H}}{H^2} = -1/3 + 2q/3$. Also, we know that $w_{tot} = \Omega_q w_q$. So, we find that

$$q = \frac{1}{2} + \frac{3}{2}\Omega_q w_q. \quad (33)$$

From the definition of the statefinder parameter r (1), it is easy to obtain

$$r = \frac{\ddot{H}}{H^3} - 3q - 2. \quad (34)$$

From Eqs. (8), (17) and (18), after some calculations, we have

$$\frac{\ddot{H}}{H^3} = \frac{9}{2} + \frac{9}{2}\Omega_q w_q (w_q + 2) - \frac{3}{2}\Omega_q w'_q + \frac{3}{2}Q_1 w_q, \quad (35)$$

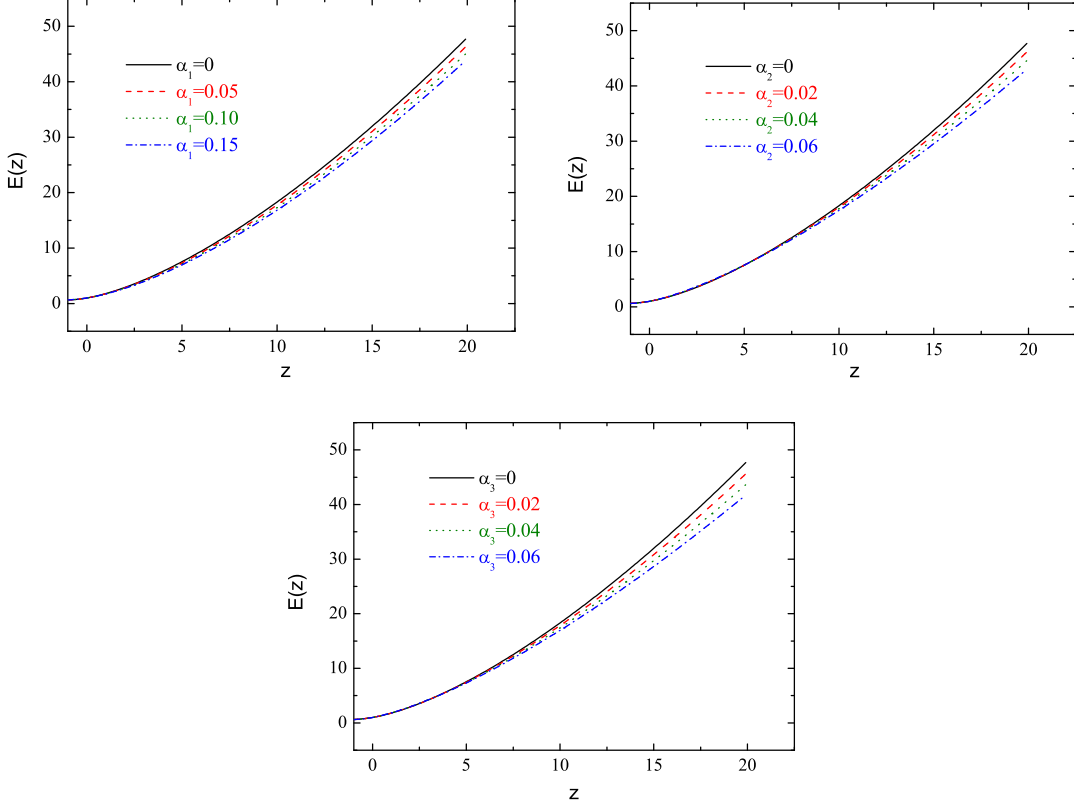


FIG. 2: The evolution of $E(z)$ for the interacting NADE model with fixed n ($n = 3$) and different interaction forms.

where

$$Q_1 = \frac{Q}{3m_p^2 H^3} = \begin{cases} 3\alpha_1 \Omega_q & \text{for } Q = 3\alpha_1 H \rho_q \\ 3\alpha_2 (1 - \Omega_q) & \text{for } Q = 3\alpha_2 H \rho_m \\ 3\alpha_3 & \text{for } Q = 3\alpha_3 H (\rho_q + \rho_m) \end{cases}. \quad (36)$$

Substituting Eqs. (33) and (35) into Eq. (34), we finally obtain

$$r = 1 + \frac{9}{2} \Omega_q w_q (1 + w_q) - \frac{3}{2} \Omega_q w'_q + \frac{3}{2} Q_1 w_q. \quad (37)$$

From the definition of the statefinder parameter s (2) and Eqs. (33), (37), it is easy to find that

$$s = 1 + w_q - \frac{w'_q}{3w_q} + \frac{Q_1}{3\Omega_q}. \quad (38)$$

From Eqs. (22) and (24), we have

$$w'_q = \frac{\sqrt{\Omega_q}}{3n} \left[(1 - \Omega_q) \left(3 - \frac{2}{na} \sqrt{\Omega_q} \right) - Q_1 \right] - Q'_2, \quad (39)$$

where Q'_2 represents the derivative of Q_2 with respect to $\ln a$, and the form of Q_2 can be written as:

$$Q_2 = \frac{Q}{3H\rho_q} = \begin{cases} \alpha_1 & \text{for } Q = 3\alpha_1 H\rho_q \\ \alpha_2 (\Omega_q^{-1} - 1) & \text{for } Q = 3\alpha_2 H\rho_m \\ \alpha_3 \Omega_q^{-1} & \text{for } Q = 3\alpha_3 H(\rho_q + \rho_m) \end{cases} . \quad (40)$$

Now the statefinder parameters r and s can be theoretically calculated for the interacting NADE model, provided that the parameters n and α_i are given. In what follows we shall plot the evolution trajectories in the statefinder planes and analyze this model from the statefinder viewpoint.

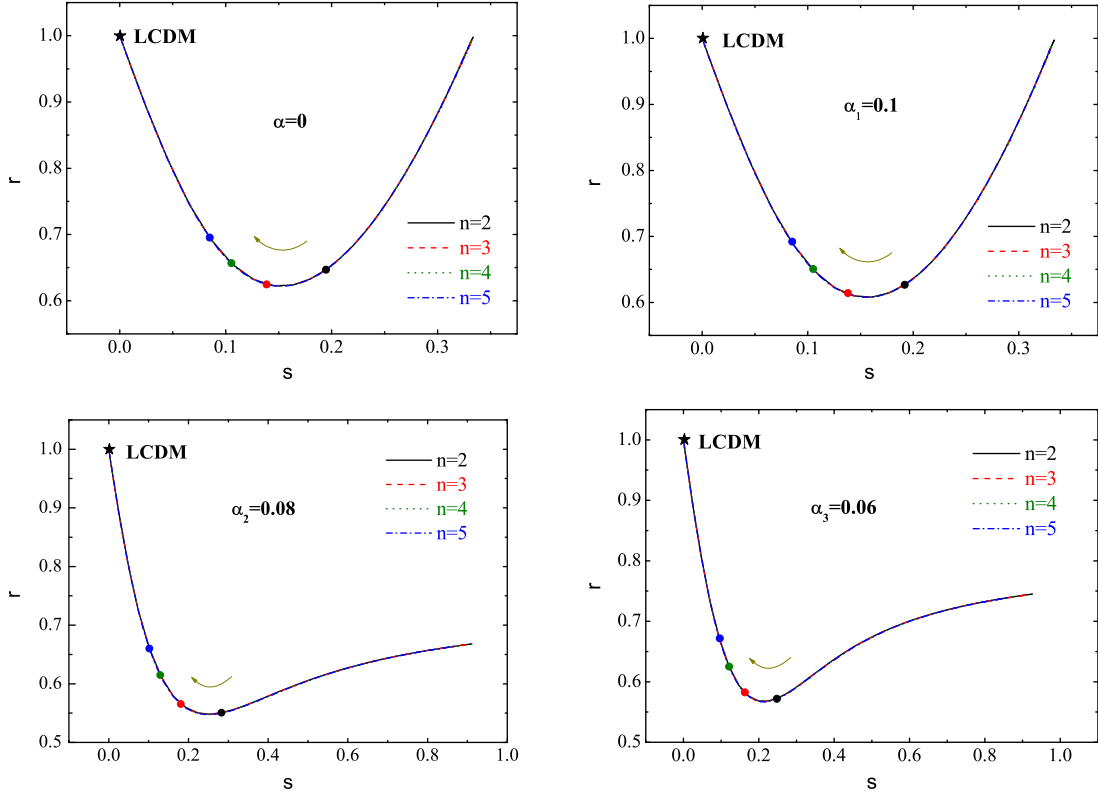


FIG. 3: The statefinder diagram $r(s)$ for the interacting NADE model with the parameter $n = 2, 3, 4$ and 5 , respectively. We take four cases without and with interactions. A star denotes the LCDM fixed point $(0, 1)$. The dots show today's values of the statefinder parameters (s_0, r_0) . It is interesting to find that the curves of each group, corresponding to different values of n , overlap together. It is also rather clear that the present values of parameters, (s_0, r_0) , are significantly distinguished because of the different values of the parameter n , though all curves end at the LCDM fixed point $(0, 1)$.

We plot the statefinder diagram in the $s - r$ planes in Figs. 3 and 4. The case $\alpha = 0$ corresponds to the case without interaction between dark energy and matter. The arrows in the diagram denote the evolution directions of the statefinder trajectories, and the star corresponds to $\{r = 1, s = 0\}$ representing the

LCDM model. In Fig. 3, we fix the interaction parameter α_i ($i = 1, 2, 3$, respectively) and vary the model parameter n . It is interesting to find that the curves of each group, corresponding to different values of n , are all degenerate. It should be mentioned that the NADE model is a single-parameter model, i.e., only the parameter n plays an important role in this model. Figure 3 shows that the present values of parameters $\{r, s\}$ are significantly distinguished because of the different values of the parameter n , though all curves end at the LCDM fixed point $\{r = 1, s = 0\}$. If the accurate information of $\{r_0, s_0\}$ can be extracted from the future high-precision observational data in a model-independent manner, the different features in this model can be discriminated explicitly by experiments, and thus one can use this method to test the NADE model as well as other dark energy models. Hence, today's values of $\{r, s\}$ play a significant role in the statefinder diagnosis. We thus calculate the present values of the statefinder parameters for different cases in the interacting NADE model and mark them on evolution curves with dots. It can be seen that the larger model parameter n results in the shorter distance from the point $\{r_0, s_0\}$ to the LCDM fixed point. In addition, in Fig. 3, the first panel with $Q = 0$ and the second one with α_1 have the similar behavior, while the situations of the third and fourth panels are similar.

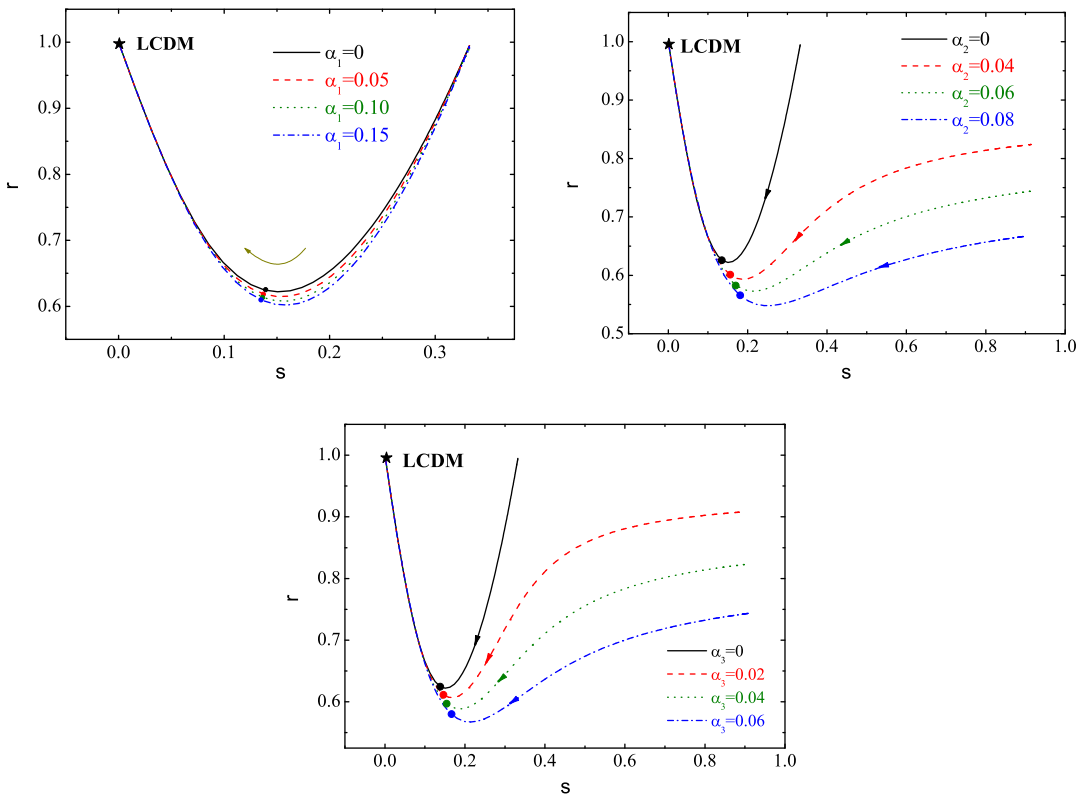


FIG. 4: The statefinder diagram $r(s)$ for the interacting NADE model with fixed n ($n = 3$) and different forms of interaction. A star denotes the LCDM fixed point $(0, 1)$. The dots show today's values of the statefinder parameters (s_0, r_0) .

We also plotted the statefinder diagram in the $s - r$ plane for different values of interaction parameter α_i with the model parameter n fixed ($n = 3$); see Fig. 4. In the left panel of Fig. 4, the interaction takes the form $Q = 3\alpha_1 H\rho_q$ with $\alpha_1 = 0, 0.05, 0.10$ and 0.15 , respectively. In the middle panel, the interaction $Q = 3\alpha_2 H\rho_m$ with $\alpha_2 = 0, 0.04, 0.06$ and 0.08 while in the right panel the interaction takes the form $Q = 3\alpha_3 H(\rho_q + \rho_m)$ with $\alpha_3 = 0, 0.02, 0.04, 0.06$, respectively. With the same value of n , we can see that the evolution trajectories for the case with interaction are tremendously distinct from that of NADE model without interaction. Moreover, the interaction of different forms will lead to different evolutionary behavior in the statefinder parameter plane. Concretely, just as we can see from the left panel of Fig. 4, when the interaction takes the form $Q = 3\alpha_1 H\rho_q$, all curves evolve from the same point to the LCDM fixed point. However, including ρ_m in the interaction Q (see the other two panels of Fig. 4), the trajectories of the interacting NADE model become very different: All curves have the same end-point (the LCDM fixed point) but they do not begin from the same point. We also calculate the present values of the statefinder parameters $\{r, s\}$ for each cases and mark them on evolutionary curves with dots in this figure. It is easy to see that the interaction will affect the today's value of statefinder parameter. For the interaction $Q = 3\alpha_1 H\rho_q$, the stronger interaction results in the shorter distance to the LCDM fixed point. For the cases with the interaction $Q = 3\alpha_2 H\rho_m$ and $Q = 3\alpha_3 H(\rho_q + \rho_m)$, the bigger value of the interaction parameter leads to the longer distance to the LCDM fixed point. From Figs. 3 and 4, we can learn that the interaction between dark components makes the value of r smaller and the value of s bigger, evidently. Also, obviously, the parameter n plays a crucial role in the interacting NADE model.

V. CONCLUDING REMARKS

In summary, we have studied the interacting NADE model from the statefinder viewpoint in this paper. Since the accelerated expansion of the universe was discovered by astronomical observations, many cosmological models have been proposed to interpret this cosmic acceleration. This leads to a problem of how to discriminate between these various contenders. The statefinder diagnosis is a useful tool for distinguishing different cosmological models by constructing the parameters $\{r, s\}$ using the higher derivative of the scale factor. Moreover, the value of $\{r, s\}$ of today can be viewed as a discriminator for testing various cosmological models if it can be extracted from precise observational data in a model-independent way. On the other hand, although we are lacking an underlying theory of dark energy, we still can make some efforts to probe the properties of dark energy according to some principle of quantum gravity. The NADE model, constructed in light of the Karolyhazy relation and corresponding energy fluctuations of space-time, is seen to possess some features of quantum gravity theory and provides us with an attempt to explore the essence

of dark energy. In addition, some physicists believe that the involvement of interaction between dark energy and dark matter leads to some alleviation and more understanding to the coincidence problem. Thus, it is worthwhile to investigate the interacting NADE model. We do this by applying the statefinder parameters as a diagnostic tool and plot the statefinder trajectories in the $s - r$ plane. We learn that the interaction between dark energy and dark matter can significantly affect the evolution of the universe, and the contribution of the interaction can be diagnosed out explicitly in this method. In addition, we show cosmological evolution of $E(z)$. For this interacting dark energy model, the parameters n and α both play important roles and thus affect the cosmological evolution. But, to determine n and α , we need more precise data provided by future experiments. We hope that the future high-precision observations can offer more and more accurate data to determine these parameters precisely and consequently shed light on the essence of dark energy.

Acknowledgements

This work was supported by the National Natural Science Foundation of China under Grant Nos.10705041 and 10975032.

-
- [1] A. G. Riess *et al.* [Supernova Search Team Collaboration], *Astron. J.* **116** (1998) 1009 [arXiv:astro-ph/9805201].
 - [2] S. Perlmutter *et al.* [Supernova Cosmology Project Collaboration], *Astrophys. J.* **517** (1999) 565 [arXiv:astro-ph/9812133].
 - [3] M. Tegmark *et al.* [SDSS Collaboration], *Phys. Rev. D* **69** (2004) 103501 [arXiv:astro-ph/0310723].
 - [4] K. Abazajian *et al.* [SDSS Collaboration], *Astron. J.* **128** (2004) 502 [arXiv:astro-ph/0403325].
 - [5] D. N. Spergel *et al.* [WMAP Collaboration], *Astrophys. J. Suppl.* **148** (2003) 175 [arXiv:astro-ph/0302209].
 - [6] C. L. Bennett *et al.* [WMAP Collaboration], *Astrophys. J. Suppl.* **148** (2003) 1 [arXiv:astro-ph/0302207].
 - [7] V. Sahni and A. A. Starobinsky, *Int. J. Mod. Phys. D* **9** (2000) 373 [arXiv:astro-ph/9904398]; P. J. E. Peebles and B. Ratra, *Rev. Mod. Phys.* **75** (2003) 559 [arXiv:astro-ph/0207347]; V. Sahni, *Lect. Notes Phys.* **653**, 141 (2004) [arXiv:astro-ph/0403324]; E. J. Copeland, M. Sami and S. Tsujikawa, *Int. J. Mod. Phys. D* **15** (2006) 1753 [arXiv:hep-th/0603057]; J. Frieman, M. Turner and D. Huterer, *Ann. Rev. Astron. Astrophys.* **46**, 385 (2008) [arXiv:0803.0982 [astro-ph]].
 - [8] V. Sahni, T. D. Saini, A. A. Starobinsky and U. Alam, *JETP Lett.* **77**, 201 (2003) [*Pisma Zh. Eksp. Teor. Fiz.* **77**, 249 (2003)] [arXiv:astro-ph/0201498].
 - [9] U. Alam, V. Sahni, T. D. Saini and A. A. Starobinsky, *Mon. Not. Roy. Astron. Soc.* **344**, 1057 (2003) [arXiv:astro-ph/0303009].
 - [10] V. Sahni, A. Shafieloo and A. A. Starobinsky, *Phys. Rev. D* **78**, 103502 (2008) [arXiv:0807.3548 [astro-ph]].
 - [11] E. Witten, hep-ph/0002297.

- [12] M. Li, Phys. Lett. B **603**, 1 (2004) [hep-th/0403127].
- [13] R. G. Cai, Phys. Lett. B **657**, 228 (2007) [arXiv:0707.4049 [hep-th]].
- [14] F. Károlyházy, Nuovo Cim. A **42**, 390 (1966); F. Károlyházy, A. Frenkel and B. Lukács, in *Physics as Natural Philosophy*, edited by A. Simony and H. Feschbach, MIT Press, Cambridge, MA (1982); F. Károlyházy, A. Frenkel and B. Lukács, in *Quantum Concepts in Space and Time*, edited by R. Penrose and C. J. Isham, Clarendon Press, Oxford, (1986).
- [15] M. Maziashvili, Int. J. Mod. Phys. D **16**, 1531 (2007) [arXiv:gr-qc/0612110].
- [16] M. Maziashvili, Phys. Lett. B **652**, 165 (2007) [arXiv:0705.0924 [gr-qc]].
- [17] H. Wei and R. G. Cai, Eur. Phys. J. C **59**, 99 (2009) [arXiv:0707.4052 [hep-th]].
- [18] H. Wei and R. G. Cai, Phys. Lett. B **660**, 113 (2008) [arXiv:0708.0884].
- [19] H. Wei and R. G. Cai, Phys. Lett. B **663**, 1 (2008) [arXiv:0708.1894].
- [20] I. P. Neupane, Phys. Rev. D **76**, 123006 (2007) [arXiv:0709.3096 [hep-th]]; M. Maziashvili, Phys. Lett. B **663**, 7 (2008) [arXiv:0712.3756 [hep-ph]]; J. Zhang, X. Zhang and H. Liu, Eur. Phys. J. C **54**, 303 (2008) [arXiv:0801.2809 [astro-ph]]; Y. W. Kim, H. W. Lee, Y. S. Myung and M. I. Park, Mod. Phys. Lett. A **23**, 3049 (2008) [arXiv:0803.0574 [gr-qc]]; J. P. Wu, D. Z. Ma and Y. Ling, Phys. Lett. B **663**, 152 (2008) [arXiv:0805.0546 [hep-th]]; J. Cui, L. Zhang, J. Zhang and X. Zhang, Chin. Phys. B (to be published), arXiv:0902.0716 [astro-ph.CO]; M. Li, X. D. Li, S. Wang and X. Zhang, JCAP **0906**, 036 (2009) [arXiv:0904.0928 [astro-ph.CO]]; X. L. Liu and X. Zhang, Commun. Theor. Phys. **52**, 761 (2009) [arXiv:0909.4911 [astro-ph.CO]].
- [21] U. Alam and V. Sahni, arXiv:astro-ph/0209443; V. Gorini, A. Kamenshchik and U. Moschella, Phys. Rev. D **67**, 063509 (2003) [arXiv:astro-ph/0209395]; W. Zimdahl and D. Pavon, Gen. Rel. Grav. **36**, 1483 (2004) [arXiv:gr-qc/0311067]; X. Zhang, F. Q. Wu and J. Zhang, JCAP **0601**, 003 (2006) [arXiv:astro-ph/0411221]; X. Zhang, Phys. Lett. B **611**, 1 (2005) [arXiv:astro-ph/0503075]; X. Zhang, Int. J. Mod. Phys. D **14**, 1597 (2005) [arXiv:astro-ph/0504586]; X. Zhang, Commun. Theor. Phys. **44**, 573 (2005); X. Zhang, Commun. Theor. Phys. **44**, 762 (2005); P. X. Wu and H. W. Yu, Int. J. Mod. Phys. D **14**, 1873 (2005) [arXiv:gr-qc/0509036]; M. G. Hu and X. H. Meng, Phys. Lett. B **635**, 186 (2006) [arXiv:astro-ph/0511615]; M. R. Setare, J. Zhang and X. Zhang, JCAP **0703**, 007 (2007) [arXiv:gr-qc/0611084]; B. R. Chang, H. Y. Liu, L. X. Xu, C. W. Zhang and Y. L. Ping, JCAP **0701**, 016 (2007) [arXiv:astro-ph/0612616]; Z. L. Yi and T. J. Zhang, Phys. Rev. D **75**, 083515 (2007) [arXiv:astro-ph/0703630]; B. Chang, H. Liu, L. Xu and C. Zhang, Mod. Phys. Lett. A **23**, 269 (2008) [arXiv:0704.3670 [astro-ph]]; J. Zhang, X. Zhang and H. Liu, Phys. Lett. B **659**, 26 (2008) [arXiv:0705.4145 [astro-ph]]; H. Wei and R. G. Cai, Phys. Lett. B **655**, 1 (2007) [arXiv:0707.4526]; W. Zhao, Int. J. Mod. Phys. D **17**, 1245 (2008) [arXiv:0711.2319 [gr-qc]]; D. J. Liu and W. Z. Liu, Phys. Rev. D **77**, 027301 (2008) [arXiv:0711.4854 [astro-ph]]; Z. G. Huang, X. M. Song, H. Q. Lu and W. Fang, Astrophys. Space Sci. **315**, 175 (2008) [arXiv:0802.2320 [hep-th]]; W. Z. Liu and D. J. Liu, Int. J. Mod. Phys. D **18**, 43 (2009) [arXiv:0803.4039 [astro-ph]]; C. J. Feng, Phys. Lett. B **670**, 231 (2008) [arXiv:0809.2502 [hep-th]]; J. Wang and S. P. Yang, arXiv:0901.1441 [gr-qc]; X. Z. Li, C. B. Sun and P. Xi, JCAP **0904**, 015 (2009) [arXiv:0903.4724 [gr-qc]]; M. L. Tong and Y. Zhang, Phys. Rev. D **80**, 023503 (2009) [arXiv:0906.3646 [gr-qc]].